

UC San Diego

UC San Diego Previously Published Works

Title

Computational simulation of JAK/STAT signaling in somatic versus germline stem cells

Permalink

<https://escholarship.org/uc/item/8hc8v9w0>

Author

Li, Willis X

Publication Date

2023-12-21

DOI

10.1002/dvdy.684

Copyright Information

This work is made available under the terms of a Creative Commons Attribution License, available at <https://creativecommons.org/licenses/by/4.0/>

Peer reviewed

Computational simulation of JAK/STAT signaling in somatic versus germline stem cells

Willis X. Li

Department of Medicine
University of California San Diego

* Corresponding author: Willis X. Li (wxli@health.ucsd.edu)

Funding

This study was supported in part by the National Institutes of Health (R01GM131044 to W.X.L).

Running title: Computational simulation of STAT signaling

Keywords: Non-canonical STAT, heterochromatin, *Drosophila*, Germline stem cell (GSC), Computer modeling

Abstract

Background: The JAK/STAT signaling pathway regulates a variety of cellular processes. A major activation event in this pathway involves the phosphorylation of a tyrosine of STAT, converting unphosphorylated STAT (uSTAT) to phosphorylated STAT (pSTAT), an active transcription factor. In a non-canonical role, uSTAT contributes to the maintenance of heterochromatin stability. As such, an increase in pSTAT concurrently reduces uSTAT, resulting in heterochromatin loss, as observed in *Drosophila* somatic tissues. Paradoxically, an opposing phenomenon occurs in *Drosophila* male germline stem cells (GSCs), where the JAK/STAT pathway remains persistently active due to a continuous supply of ligands. Here, computational simulations were employed to dissect JAK/STAT pathway activation under different cellular contexts, mimicking somatic and germline cells. In these simulations, ordinary differential equations were leveraged to replicate the chemical reactions governing JAK/STAT signaling under different conditions.

Results: The outcomes indicate that transient ligand stimulation, typical in somatic tissues, led to a momentary reduction in uSTAT levels. Conversely, sustained ligand stimulation, a characteristic feature of the GSC niche, resulted in elevated uSTAT levels at equilibrium.

Conclusion: The simulation suggests that the duration of ligand exposure could explain the observed opposite effects of JAK/STAT activation on heterochromatin in somatic versus germline stem cells.

Introduction

The canonical Janus kinase/Signal Transducer and Activator of Transcription (JAK/STAT) pathway is activated when extracellular ligands, such as cytokines or growth factors, bind to cell surface receptors. This triggers intracellular JAK activation, leading to the phosphorylation and activation of STAT proteins, which subsequently translocate to the nucleus, orchestrating the expression of target genes¹⁻³. In *Drosophila*, the JAK/STAT pathway comprises several key components, including the interleukin-like ligands Unpaired (Upd) proteins, a membrane receptor Domeless (Dome), a single JAK kinase Hopscotch (Hop), and a single STAT protein, STAT92E^{2, 4-6}. This canonical JAK/STAT pathway is auto-regulated by negative feedback mechanisms, involving negative regulators such as Protein Tyrosine Phosphatase (PTP), Suppressor of Cytokine Signaling (SOCS), and Protein Inhibitors of Activated STAT (PIAS) family proteins^{2, 4-6} (**Figure 1**). In *Drosophila*, two STAT target genes, *Socs36E* and *Ptp61F*, have been identified as negative regulators of JAK/STAT signaling, forming a critical negative feedback loop⁷⁻⁹. These negative regulators contribute to the autoregulation of the JAK/STAT pathway, with PTP61F, in particular, dephosphorylating tyrosine residues of JAK and STAT⁷, thereby modulating the balance between pSTAT and uSTAT.

Previous studies have uncovered noncanonical JAK/STAT signaling, where JAK activation counteracts heterochromatin formation in *Drosophila*^{10, 11} and in human leukemia and stem cells¹²⁻¹⁵. It has been demonstrated that a portion of unphosphorylated STAT (uSTAT) proteins reside in the nucleus in association with Heterochromatin Protein 1 (HP1), thereby stabilizing heterochromatin formation. Conversely, STAT activation through phosphorylation leads to its dispersal, resulting in HP1 delocalization and heterochromatin loss^{2, 16}. Therefore, the concentration of uSTAT is particularly important for regulating heterochromatin formation as a non-canonical STAT function^{10, 16}.

The JAK/STAT pathway serves numerous biological functions and is essential for the maintenance of *Drosophila* male germline stem cells (GSCs), which offers a valuable model for the study of stem cell regulation¹⁷⁻²¹. In *Drosophila* testis, hub cells, known as the GSC niche, continuously secrete the ligand Upd, resulting in the sustained activation of the JAK/STAT

pathway in GSCs and somatic cyst stem cells (CySCs), instructing their self-renewal. Studies have shown that overexpression of Upd greatly increases GSC number, whereas *hop* loss-of-function mutant flies lose all GSCs in testes and are male sterile, and GSCs that have lost *stat92E* are unable to self-renewal²². Although later studies have shown that JAK/STAT activation is required not in GSCs, but rather in the adjacent somatic CySCs, which in turn maintains GSCs, and that STAT activation in GSCs functions to merely ensure their adhesion to the hub^{23, 24}, contrasting studies have shown that CySCs are dispensable for GSC maintenance²⁵, and that JAK/STAT activation in GSCs is required for their maintenance^{26, 27}, possibly through regulating cytokinesis²⁸. Moreover, it has been shown that STAT is required in GSCs for male sex identity through Phf7²⁹, for adhesion to the niche through E-Cadherin²⁴, for GSC survival³⁰, and for F-actin regulation in GSCs³¹. Recent research has further highlighted the necessity of both canonical and non-canonical functions of STAT in GSC maintenance, in part, through regulating heterochromatin formation³².

As the stem cell niche, hub cells at the testis tip region provide a continuous supply of Upd ligand, resulting in sustained JAK/STAT pathway stimulation in adjacent GSCs and CySCs^{22, 33}. In somatic tissues, however, JAK/STAT is activated only under certain physiological situations, by transient increases in ligands. Paradoxically, in somatic tissues, transient activation of JAK/STAT signaling decreases heterochromatin^{10, 16}, whereas sustained activation of JAK/STAT signaling in GSCs increases heterochromatin formation³². This paradoxical observation raises the possibility that the JAK/STAT pathway may operate differently in somatic vs. germline cells, possibly due to differences in pathway components or regulators. The present study employed mathematical simulations to elucidate how activation of the JAK/STAT pathway in the germline vs somatic cells could result in different biological consequences. Ordinary differential equations and known physiological concentrations of JAK/STAT components were used to simulate the chemical reactions of the canonical STAT pathway activation under different durations of ligand stimulation. These simulations unveiled that transient ligand exposure led to a momentary decrease in uSTAT levels, known to decrease heterochromatin formation. Conversely, sustained ligand exposure culminated in elevated uSTAT levels at equilibrium, promoting heterochromatin formation. These results suggest that the duration of ligand supply alone could account for the observed differences in heterochromatin regulation in somatic and germline stem cells.

Results

The JAK/STAT regulatory network used in simulation

To computationally simulate JAK/STAT signaling in somatic vs germline tissues of *Drosophila*, a simplified signaling network was employed, which consisted of the core components of the pathway – a ligand Unpaired (Upd), a receptor (R), a JAK, a STAT, and two negative regulators, PTP and a SOCS. The regulatory relationships among the components of this simplified canonical JAK/STAT pathway are schematically shown (**Figure 1A**). This network of regulatory components functioned to control the levels and balance of unphosphorylated STAT (uSTAT) and phosphorylated (pSTAT), with the latter being the active transcription factor. In addition to uSTAT itself, transcriptional induction of the negative regulators PTP and SOCS depended on the level of pSTAT, establishing a feedback regulatory loop (**Figure 1B**).

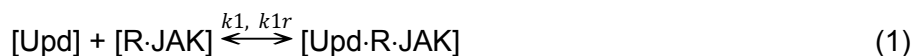
For simulation purposes, activation of the JAK/STAT pathway is initiated by Upd binding to R, leading to the formation of activated or phosphorylated JAK (pJAK), which then binds to uSTAT and catalyzes its conversion into pSTAT. The simulated protein-protein interactions and signaling events take place in a single compartment, obviating the need for translocation between the cytoplasm to the nucleus. Furthermore, processes such as cell division or growth in volume were not considered due to the short time scale relevant to computer modeling. While it is acknowledged that Protein Inhibitors of Activated STAT (PIAS) also serve as negative

regulators of the JAK/STAT pathway³⁴, their transcription regulation remains unclear and, thus, was not included in the simplified regulatory network. Lastly, SOCS, which inhibits JAK/STAT signaling by associating with and sequestering pJAK, was integrated into the streamlined version of the signaling network. This simplified signaling network encompasses all essential components and regulatory mechanisms of the JAK/STAT pathway.

Chemical reactions and kinetics

The chemical reaction equations in modeling were derived from established knowledge of the canonical JAK/STAT pathway in both *Drosophila* and human cells³⁵. Ordinary differential equations (ODEs) were formulated based on the chemical reaction equations to describe the dynamic changes in the pathway components.

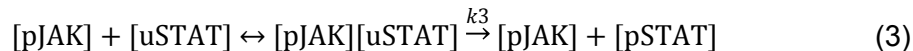
The system is initiated when the ligand Upd is bound to a Receptor-JAK complex [R][JAK] in a reversible reaction (eq 1), with a forward rate constant k_1 and a reverse rate constant k_{1r} .



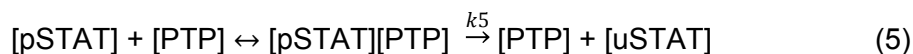
The association of Upd with the Receptor-JAK complex leads to the formation of phosphorylated JAK (pJAK). Since phosphorylation is a covalent modification, this process is described as an irreversible reaction (eq 2), with a rate constant k_2 .



Similarly, the reversible binding of uSTAT to pJAK results in the phosphorylation of uSTAT, converting it to pSTAT in an irreversible reaction (eq 3), with a rate constant k_3 .



In addition, pSTAT and pJAK can be dephosphorylated by the protein phosphatase PTP, resulting in the conversion of pSTAT to uSTAT and pJAK to JAK. These are irreversible reactions (eq 4-5) with rate constants k_4 and k_5 .



Lastly, SOCS inhibits pJAK by directly binding to pJAK or the receptor-pJAK complex, forming an inactive complex, thereby blocking the protein kinase activity toward STAT³⁶. The reversible reaction is described in (eq 6) with forward and reverse rate constants k_6 and k_{6r} .



The above protein-protein interactions, chemical reactions, and kinetics were incorporated to derive a set of ODEs in the following to describe how the concentrations of the signaling components dynamically change over time. For example, the binding of the ligand Upd leading to the formation of the Upd-R-JAK complex is described in the following ODE (eq 7).

$$\frac{d[Upd \cdot R \cdot JAK]}{dt} = k1 \cdot [Upd][R \cdot JAK] - k1r \cdot [Upd \cdot R \cdot JAK] - k2 \cdot [Upd \cdot R \cdot JAK], \quad (7)$$

where the first two terms represent association and dissociation between Upd and R·JAK; and the third term is the loss of the Upd·R·JAK complex due to pJAK formation, as described in Eq.2.

The complex Upd·R·JAK formation leads to the phosphorylation of JAK, producing pJAK, which is described in the following ODE (eq 8).

$$\frac{d[pJAK]}{dt} = k2 \cdot [Upd \cdot R \cdot JAK] - k4 \cdot [pJAK][PTP] - k6 \cdot [pJAK][SOCS] + k6r \cdot [pJAK \cdot SOCS], \quad (8)$$

where the first term is the rate of pJAK production, as described above; the second term describes the loss of pJAK due to dephosphorylation by PTP, an irreversible process; and the third and fourth terms describe the reversible association between pJAK and SOCS, sequestering pJAK.

Phosphorylation of uSTAT to form pSTAT is an important step in JAK/STAT signaling, which can be described in the following ODE (eq 9).

$$\frac{d[pSTAT]}{dt} = k3 \cdot [pJAK][uSTAT] - a1 \cdot [pSTAT] - k5 \cdot [PTP][pSTAT], \quad (9)$$

where the first term describes the rate of pSTAT production from the pJAK·uSTAT complex; the second term represents pSTAT degradation; and the third term for the irreversible dephosphorylation of pSTAT.

Since pSTAT functions as a transcription factor capable of inducing its own expression (autoregulation), the rate of uSTAT synthesis is dependent on the concentration of pSTAT dimers, which is half of pSTAT monomer concentration, as described by the following differential equation (Eq.10).

$$\frac{d[uSTAT]}{dt} = \frac{a2 \cdot [pSTAT]}{2} + a3 - a4 \cdot [uSTAT] + k5 \cdot [pSTAT][PTP] - k3 \cdot [pJAK][uSTAT], \quad (10)$$

where the first term represents the increase of uSTAT due to pSTAT dimer-dependent transcription, with rate proportionality constant a2. The second term represents a basal level of uSTAT production, at rate a3, which is not regulated by pSTAT. The third term represents uSTAT degradation, with rate constant a4. The fourth term represents the formation of uSTAT from pSTAT dephosphorylation.

Since the transcriptional regulation of PTP depends on pSTAT, as described in the following ODE equation.

$$\frac{d[PTP]}{dt} = \frac{a5 \cdot [pSTAT]}{2} + p - a6 \cdot [PTP] \quad (11)$$

where a5 is the rate constant of pSTAT-dependent PTP synthesis; a6 represents the rate constant for PTP degradation. p represents a basal level PTP production independent of pSTAT.

Similarly, the transcriptional regulation of SOCS also depends on pSTAT dimer concentration, as described in the following ODE equation.

$$\frac{d[SOCS]}{dt} = \frac{a7 \cdot [pSTAT]}{2} + s - a8 \cdot [SOCS] - k6 \cdot [pJAK][SOCS] + k6r \cdot [pJAK \cdot SOCS], \quad (12)$$

where $a5$ is the rate constant of pSTAT-dependent SOCS synthesis; $a6$ represents the rate constant for SOCS degradation. s represents a basal level SOCS production independent of pSTAT. In addition, The last two terms describe changes in SOCS concentration as it reversibly associates with pJAK.

Lastly, changes in SOCS-pJAK complex formation is described in the following ODE equation,

$$\frac{d[pJAK \cdot SOCS]}{dt} = k6 \cdot [pJAK][SOCS] - k6r \cdot [pJAK \cdot SOCS], \quad (13)$$

where $k6$ and $k6r$ are the forward and reverse rate constants, as in Eq. 6.

Simulation of JAK/STAT signaling with different Upd duration

The above set of ODEs, representing the kinetics of JAK/STAT signaling pathway, was used for simulation with MATLAB. The kinetic parameters (rate constants) and initial concentrations were from previous reports of the human JAK/STAT pathway^{35, 37}, or were arbitrarily chosen to derive an activation curve based on known characteristics of the JAK/STAT pathway. The initial concentrations of uSTAT, PTP, and SOCS were set at 10, 1, and 1 nM, respectively. JAK and R concentrations were maintained at constant levels with slow production and turnover rates unaffected by signaling activities, whereas the levels of uSTAT, PTP, and SOCS are additionally regulated by JAK/STAT signaling, as previously reported^{2, 4-6}.

To validate the selection of parameters, a parameterization analysis was conducted with varying time intervals and concentrations of Upd to assess the pathway's sensitivity and stability to ligand stimulation. Various scenarios were tested, comparing the time course of stimulating the pathway with Upd concentrations at 0.1, 1, 5, and 10 nM for durations of 1, 5, 10, and 20 minutes. The analysis revealed that Upd concentration and duration primarily influenced the magnitude of pJAK and pSTAT formation. Importantly, after stimulation in each scenario, the levels of uSTAT and other components returned to pre-stimulation levels when the system reached equilibrium (**Figure 2**), demonstrating that the signaling pathway modeled with the chosen parameters exhibits robustness and stability. It could tolerate large variations in the quantity or duration of stimulation. For subsequent analyses, Upd stimulation at 1 nM for 10 minutes was chosen.

The dynamics of JAK/STAT signaling were simulated under two distinct conditions: pulsed ligand stimulation, representing what occurs in somatic tissues (except for CySCs), and sustained ligand stimulation, mimicking the situation in the GSC niche, where CySCs are also present but indistinguishable from GSCs in this model.

Results from the simulations indicate that a pulse of Upd ligand stimulation initially increases pSTAT levels, while decreasing uSTAT levels, and pSTAT and uSTAT will return to steady-state concentrations over time (**Figure 3A**). However, when Upd is present constantly, as in the GSC niche, cells can maintain a 2-fold elevated uSTAT level at equilibrium (from 10.0 to 19.2 nM) (**Figure 3B**). In both cases, ligand Upd engagement causes an initial peak of pSTAT and a simultaneous significant drop in uSTAT levels. This initial reduction in uSTAT levels could potentially destabilize heterochromatin, which aligns with prior observations in somatic tissues¹⁶. However, the sustained elevation of uSTAT levels seen in GSCs could promote heterochromatin formation. This simulation is consistent with observations of high STAT levels in GSCs detected with antibodies specific for total STAT92E^{23, 29, 38-40} and the presence of high levels of heterochromatin important for GSC maintenance^{32, 41}. Thus, sustained activation of the

JAK/STAT pathway, as occurs in GSCs, can lead to the accumulation of high levels of uSTAT, which favors heterochromatin formation.

Effects of JAK mutations on the system output

In *Drosophila*, the JAK kinase is encoded by the gene *hopscotch* (*hop*), located on the X chromosome⁴². The hypomorphic loss-of-function *hop* mutant allele *hop*²⁵ carries a Q246K mutation within the JH6 domain, presumably reducing its kinase activity⁴³, presumably causing physiological consequences including lethality. Indeed, hemizygous *hop*²⁵ males usually do not survive to the adult stage, and the rare escapers are sterile with reduced testes and loss of GSCs.

In simulating JAK/STAT signaling in *hop*²⁵ mutants, the forward rate constant k_2 in eq. 2 was lowered by 100-fold to reflect a much slower rate of formation of functional pJAK, while all other parameters remained unchanged. With a slower rate of pJAK formation, the same Upd stimulation had little effects in somatic cells, such that uSTAT and pSTAT were little changed (**Figure 4A**), consistent with the lack of JAK/STAT signaling in *hop*²⁵ mutant animals. In GSCs, which receive sustained Upd stimulation, there was a slight increase in both uSTAT and pSTAT levels (**Figure 4B**). However, the levels of uSTAT and pSTAT are much lower than in wild-type GSCs, consistent with the sterile phenotype of *hop*²⁵ mutant male escapers.

On the other hand, the *tumorous-lethal* allele, *hop*^{Tum-I}, is a gain-of-function mutation due to a G341E amino acid replacement, resulting in a hyperactive JAK kinase⁴⁴⁻⁴⁶. Although the molecular mechanism remains unclear, the G341E substitution may disrupt negative autoregulation and make activation by phosphorylation easier. One way to simulate the *hop*^{Tum-I} mutation is to increase the forward rate constant k_2 in eq. 2 by 100-fold to reflect a much higher rate of pJAK formation in response to Upd, while keeping all other parameters unchanged. In somatic cells with pulsed Upd stimulation, this mutation resulted in an initial decrease of uSTAT levels by 95%, followed by a spike before returning to normal levels (**Figure 5A**). The steeper initial drop in uSTAT levels might account for the heterochromatin disruption observed in somatic tissues of *hop*^{Tum-I} mutants¹⁰. In contrast, in GSCs with sustained Upd stimulation, this mutation led to a 2.5-fold elevated uSTAT level to 24.6 nM at steady state, despite a similar initial decrease (**Figure 5B**), consistent with the observed higher uSTAT levels heterochromatin levels in GSCs³². GSCs having higher levels of uSTAT, as detected by antibodies against total STAT, have been previously reported³⁸⁻⁴⁰.

Alternatively, the *hop*^{Tum-I} mutation could lead to constitutive activation of JAK regardless of Upd stimulation. To simulate this scenario, pJAK is supplied at a constant 3 nM. Since the difference in Upd production is now irrelevant, certain parameters need to be adjusted to differentiate somatic cells from GSCs. If the rate of uSTAT degradation is slower by half in GSCs ($a_4=0.5$) than in somatic cells ($a_4=1.0$), a constant presence of pJAK led to a high concentration of uSTAT (36.4 nM) in GSCs at equilibrium, as compared with a low concentration of uSTAT (2.9 nM) in somatic cells (**Figure 6A**). On the other hand, if the rate of PTP synthesis was adjusted to be slower in GSCs ($a_5=1.0$) than in somatic cells ($a_5=10$), a constant presence of pJAK resulted in a high concentration of uSTAT (37.0 nM) in GSCs, as compared with a low concentration of uSTAT (5.3 nM) in somatic cells (**Figure 6B**). In either scenario, GSCs would contain much higher uSTAT and somatic cells would have lower levels of uSTAT than in normal situations. These differences could also account for the lower heterochromatin in somatic cells and high heterochromatin in GSCs in *hop*^{Tum-I} mutant flies. Future experimental validation would be essential to confirm the actual mechanisms at play in these scenarios.

Discussion

Computer simulations were employed to explore the dynamics of the JAK/STAT pathway in wildtype, *hop* gain-of-function, and loss-of-function mutants within somatic and germline tissues. Paradoxical observations have been documented in germline and somatic cells. In somatic cells, JAK activation is known to reduce heterochromatin, while germline stem cells (GSCs) exhibit higher heterochromatin levels due to active JAK/STAT signaling sustained by continuous Upd secretion from the niche. Additionally, GSCs accumulate higher STAT levels compared to somatic cells. These disparities have led to speculations about differential behavior of the JAK/STAT pathway in germline versus somatic cells. However, my simulations indicate that variations in the extracellular ligand stimulation mode, rather than differences in signaling components, can explain these distinct JAK/STAT signaling outcomes.

The simulations were based on the premise that GSCs receive constant Upd stimulation secreted by hub cells in the GSC niche^{22, 33}, while somatic cells, excluding CySCs, encounter transient Upd production in response to various physiological cues, such as immune reactions. Although CySCs, due to their small size, haven't undergone comprehensive examination regarding heterochromatin content, they reside in the same microenvironment as GSCs and receive Upd signals similarly. It's possible that CySCs also possess elevated heterochromatin levels. The simulations were conducted using a set of ordinary differential equations derived from the chemical reactions governing the JAK/STAT signaling pathway. The results revealed that sustained Upd production leads to higher uSTAT levels at equilibrium, corroborating the observations of GSCs containing substantial uSTAT levels. Conversely, transient Upd production results in a temporary reduction of uSTAT, resembling the behavior in somatic tissues. Results from these simulations are consistent with the observation that GSCs contain high levels of uSTAT^{23, 29, 38-40}.

It has been previously shown that both canonical and noncanonical functions of JAK/STAT signaling in GSCs are important for GSC maintenance³². Moreover, it has been shown that the central heterochromatin components such as HP1 and Su(var)3-9 methyltransferase are required for GSC maintenance⁴¹ and that GSCs have higher levels of heterochromatin, which is regulated by the non-canonical STAT function. Further, both HP1 and STAT are among the transcription targets of canonical JAK/STAT signaling in GSCs. Thus, canonical and noncanonical functions of JAK/STAT signaling together regulate heterochromatin formation for GSC maintenance³².

Computer simulations in the current study indicate that, in wild-type animals, the mode of Upd stimulation alone, without necessitating alterations in other signaling components or parameters, can predict the distinct outcomes of JAK/STAT signaling in germline vs somatic cells. Continuous Upd supply results in higher levels of uSTAT at equilibrium, as observed in GSCs, while pulsed Upd production results in a transitory decrease of uSTAT, followed by a return to normal unstimulated levels. This transitory decrease in uSTAT levels in somatic cells might cause a disruption in heterochromatin formation, while sustained high levels of uSTAT in GSCs might compensate for the initial decrease in uSTAT and lead to increased heterochromatin formation.

It is important to acknowledge that the simulations in this study employed a simplified model of JAK/STAT signaling. While this simplification streamlines calculations, it may not consistently capture the intricacies of the actual cellular processes. For instance, the assumption of pSTAT dimer concentration being half of pSTAT monomer concentration for simplifying pSTAT dimerization oversimplifies reality, as not all pSTAT molecules exist in dimer form. Dimerization of pSTAT monomers should ideally follow thermodynamic reactions with associated rate constants, akin to other protein-protein interactions. Consequently, a comprehensive simulation that considers all chemical reactions might entail greater complexity than the streamlined version adopted in this study.

Furthermore, by modifying the rate of pJAK production, gain-of-function (*hop^{Tum-I}*) and loss-of-function (*hop²⁵*) mutants were simulated. Although these mutations may impact various

aspects of JAK protein, including protein stability and conformation, they ultimately influence the availability of functional pJAK. Thus, the rate of pJAK formation was adjusted in the simulations to simplify the scenarios related to different *hop* mutations. The simulation results indicated that increasing the pJAK production rate leads to a more pronounced initial uSTAT loss in cells, consistent with previous findings associated with the gain-of-function *hop^{Tum-I}* mutation¹⁰. Notably, in GSCs subjected to the same gain-of-function JAK alteration, steady-state uSTAT levels are higher, a phenomenon previously linked to enhanced heterochromatin formation^{2, 16}. Although an initial loss of uSTAT after stimulation occurs in all scenarios, it is reasonable to speculate that the final steady-state uSTAT level plays a pivotal role in determining whether the initial loss uSTAT can be compensated for, influencing the ultimate heterochromatin content in cells. Additionally, the presence of steady-state pJAK in GCSs would increase the levels of HP1, a STAT target gene³², further promoting heterochromatin formation. This interpretation aligns with the observed higher heterochromatin content in *Drosophila* male GSCs³². Future studies are warranted to uncover the biological functions of heterochromatin in adult stem cell maintenance.

Experimental Procedures

Computer simulation of JAK/STAT signaling

The JAK/STAT pathway was simulated using the MATLAB ODE45 function in MATLAB® Online™ (R2023a) to solve the first-order ordinary differential equations (ODEs) based on chemical reactions described in the text. The following initial conditions or concentrations (nM) were used. $[R \cdot JAK]_0 = 0.2$; $[uSTAT]_0 = 10$; $[PTP]_0 = 1$; $[SOCS]_0 = 1$; Other molecules were set to 0 initiation concentration. The system was run from 0 to 300 min to reach equilibrium. The ligand Upd (1 nM) was added to the system at 30 min for 10 min (pulsed stimulation) or for the whole remaining duration (sustained stimulation). First-order forward (k) and reverse (k_r) rate constants are expressed in m^{-1} . The following rate constants were used. $k_1 = 20$; $k_{r1} = 0.2$; $k_2 = 0.1$; $k_3 = 1$; $k_4 = 0.1$; $k_5 = 0.01$; $k_6 = 20$; $k_{r6} = 0.1$; $a_1 = 0.01$; $a_2 = 0.05$; $a_3 = 0.2$; $a_4 = 0.02$; $a_5 = 0.05$; $p = 0.01$; $a_6 = 0.01$; $a_7 = 0.05$; $s = 0.005$; $a_8 = 0.005$.

Acknowledgments

I thank members of the Li lab for helpful discussions

Data sharing statement

All supporting data are included within the main article and its supplementary files.

Conflict of Interest Statement

The author declares no conflict of interest.

Figure Legends

Figure 1. JAK/STAT signaling components and network used for simulation

(A) Schematic representation of simplified JAK/STAT signaling pathway components and their regulatory relationships. (B) Transcription factor pSTAT induces the expression of target genes uSTAT, SOCS, and PTP.

Figure 2. Parameterization analysis for JAK/STAT signaling simulation

Changes in concentrations of the indicated JAK/STAT signaling pathway components over time (from 0 to 300 minutes) are shown following the addition of the ligand Upd at different concentrations and durations, as indicated.

Figure 3. Simulated JAK/STAT signaling in wild-type somatic and germline stem cells

Changes in concentrations of the indicated JAK/STAT signaling pathway components over time (from 0 to 300 minutes) are shown. [uSTAT] at 300 min is indicated. (A) somatic cells: 1 nM Upd was added at time 30 min for a duration of 10 min. (B) GSCs: 1 nM Upd was added at time 30 min for the remaining time.

Figure 4. Simulated JAK/STAT signaling in *hop* loss-of-function mutants

Changes in concentrations of the indicated JAK/STAT signaling pathway components over time (from 0 to 300 minutes) are shown. In *hop* loss-of-function mutants, the rate of functional pJAK formation is 100-fold slower than in the wild type. (A) somatic cells: 1 nM Upd was added at time 30 min for a duration of 10 min. (B) GSCs: 1 nM Upd was added at time 30 min for the remaining time.

Figure 5. Simulated JAK/STAT signaling in *hop* gain-of-function mutants

Changes in concentrations of the indicated JAK/STAT signaling pathway components over time (from 0 to 300 minutes) are shown. In *hop* gain-of-function mutants, the rate of functional pJAK formation is 100-fold faster than in the wild type. (A) somatic cells: 1 nM Upd was added at time 30 min for a duration of 10 min. (B) GSCs: 1 nM Upd was added at time 30 min for the remaining time.

Figure 6. Alternative simulations of JAK/STAT signaling in *hop* gain-of-function mutants

Changes in concentrations of the indicated JAK/STAT signaling pathway components over time (from 0 to 300 or 600 minutes) are shown without Upd exposure. (A) The rate constant for uSTAT degradation is 1 in somatic cells vs 0.5 in GSCs. (B) The rate constant for PTP synthesis is 10 in somatic cells vs 1 in GSCs. [uSTAT] at equilibrium is indicated

References

- (1) Yu, H.; Pardoll, D.; Jove, R. STATs in cancer inflammation and immunity: a leading role for STAT3. *Nat Rev Cancer* **2009**, *9* (11), 798-809, Review. DOI: 10.1038/nrc2734.
- (2) Li, W. X. Canonical and non-canonical JAK-STAT signaling. *Trends Cell Biol* **2008**, *18* (11), 545-551.
- (3) Philips, R. L.; Wang, Y.; Cheon, H.; Kanno, Y.; Gadina, M.; Sartorelli, V.; Horvath, C. M.; Darnell, J. E.; Stark, G. R.; O'Shea, J. J. The JAK-STAT pathway at 30: Much learned, much more to do. *Cell* **2022**, *185* (21), 3857-3876. DOI: 10.1016/j.cell.2022.09.023.
- (4) Xi, R.; McGregor, J. R.; Harrison, D. A. A gradient of JAK pathway activity patterns the anterior-posterior axis of the follicular epithelium. *Dev Cell* **2003**, *4* (2), 167-177.
- (5) Arbouzova, N. I.; Zeidler, M. P. JAK/STAT signalling in Drosophila: insights into conserved regulatory and cellular functions. *Development* **2006**, *133* (14), 2605-2616.
- (6) Rawlings, J. S.; Rosler, K. M.; Harrison, D. A. The JAK/STAT signaling pathway. *J Cell Sci* **2004**, *117* (Pt 8), 1281-1283.
- (7) Baeg, G. H.; Zhou, R.; Perrimon, N. Genome-wide RNAi analysis of JAK/STAT signaling components in Drosophila. *Genes Dev* **2005**, *19* (16), 1861-1870.
- (8) Callus, B. A.; Mathey-Prevot, B. SOCS36E, a novel Drosophila SOCS protein, suppresses JAK/STAT and EGF-R signalling in the imaginal wing disc. *Oncogene* **2002**, *21* (31), 4812-4821. DOI: 10.1038/sj.onc.1205618.
- (9) Muller, P.; Kutteneuler, D.; Gesellchen, V.; Zeidler, M. P.; Boutros, M. Identification of JAK/STAT signalling components by genome-wide RNA interference. *Nature* **2005**, *436* (7052), 871-875.
- (10) Shi, S.; Calhoun, H. C.; Xia, F.; Li, J.; Le, L.; Li, W. X. JAK signaling globally counteracts heterochromatic gene silencing. *Nat Genet* **2006**, *38* (9), 1071-1076.
- (11) Betz, A.; Darnell, J. E., Jr. A Hopscotch-chromatin connection. *Nat Genet* **2006**, *38* (9), 977-979.
- (12) Dawson, M. A.; Bannister, A. J.; Gottgens, B.; Foster, S. D.; Bartke, T.; Green, A. R.; Kouzarides, T. JAK2 phosphorylates histone H3Y41 and excludes HP1alpha from chromatin. *Nature* **2009**, *461* (7265), 819-822, Research Support, Non-U.S. Gov't. DOI: 10.1038/nature08448.
- (13) Griffiths, D. S.; Li, J.; Dawson, M. A.; Trotter, M. W.; Cheng, Y. H.; Smith, A. M.; Mansfield, W.; Liu, P.; Kouzarides, T.; Nichols, J.; et al. LIF-independent JAK signalling to chromatin in embryonic stem cells uncovered from an adult stem cell disease. *Nat Cell Biol* **2011**, *13* (1), 13-21, Research Support, Non-U.S. Gov't. DOI: 10.1038/ncb2135.
- (14) Rui, L.; Emre, N. C.; Kruhlak, M. J.; Chung, H. J.; Steidl, C.; Slack, G.; Wright, G. W.; Lenz, G.; Ngo, V. N.; Shaffer, A. L.; et al. Cooperative epigenetic modulation by cancer amplicon genes. *Cancer Cell* **2010**, *18* (6), 590-605. DOI: 10.1016/j.ccr.2010.11.013.
- (15) Rui, L.; Drennan, A. C.; Ceribelli, M.; Zhu, F.; Wright, G. W.; Huang, D. W.; Xiao, W.; Li, Y.; Grindle, K. M.; Lu, L.; et al. Epigenetic gene regulation by Janus kinase 1 in diffuse large B-cell lymphoma. *Proc Natl Acad Sci U S A* **2016**, *113* (46), E7260-E7267. DOI: 10.1073/pnas.1610970113.
- (16) Shi, S.; Larson, K.; Guo, D.; Lim, S. J.; Dutta, P.; Yan, S. J.; Li, W. X. Drosophila STAT is required for directly maintaining HP1 localization and heterochromatin stability. *Nat Cell Biol* **2008**, *10* (4), 489-496.
- (17) Lin, H. The stem-cell niche theory: lessons from flies. *Nat Rev Genet* **2002**, *3* (12), 931-940. DOI: 10.1038/nrg952
nrg952 [pii].
- (18) Fuller, M. T.; Spradling, A. C. Male and female Drosophila germline stem cells: two versions of immortality. *Science* **2007**, *316* (5823), 402-404.

- (19) Morrison, S. J.; Spradling, A. C. Stem cells and niches: mechanisms that promote stem cell maintenance throughout life. *Cell* **2008**, *132* (4), 598-611.
- (20) de Cuevas, M.; Matunis, E. L. The stem cell niche: lessons from the *Drosophila* testis. *Development* **2011**, *138* (14), 2861-2869. DOI: 10.1242/dev.056242.
- (21) Bausek, N. JAK-STAT signaling in stem cells and their niches in *Drosophila*. *JAKSTAT* **2013**, *2* (3), e25686. DOI: 10.4161/jkst.25686.
- (22) Tulina, N.; Matunis, E. Control of stem cell self-renewal in *Drosophila* spermatogenesis by JAK-STAT signaling. *Science* **2001**, *294* (5551), 2546-2549.
- (23) Leatherman, J. L.; Dinardo, S. Zfh-1 controls somatic stem cell self-renewal in the *Drosophila* testis and nonautonomously influences germline stem cell self-renewal. *Cell Stem Cell* **2008**, *3* (1), 44-54.
- (24) Leatherman, J. L.; Dinardo, S. Germline self-renewal requires cyst stem cells and stat regulates niche adhesion in *Drosophila* testes. *Nat Cell Biol* **2010**, *12* (8), 806-811. DOI: ncb2086 [pii] 10.1038/ncb2086.
- (25) Lim, J. G.; Fuller, M. T. Somatic cell lineage is required for differentiation and not maintenance of germline stem cells in *Drosophila* testes. *Proc Natl Acad Sci U S A* **2012**, *109* (45), 18477-18481. DOI: 10.1073/pnas.1215516109.
- (26) Tarayrah, L.; Li, Y.; Gan, Q.; Chen, X. Epigenetic regulator Lid maintains germline stem cells through regulating JAK-STAT signaling pathway activity. *Biol Open* **2015**, *4* (11), 1518-1527. DOI: 10.1242/bio.013961.
- (27) Chen, C.; Cummings, R.; Mordovanakis, A.; Hunt, A. J.; Mayer, M.; Sept, D.; Yamashita, Y. M. Cytokine receptor-Eb1 interaction couples cell polarity and fate during asymmetric cell division. *Elife* **2018**, *7*. DOI: 10.7554/eLife.33685.
- (28) Lenhart, K. F.; Capozzoli, B.; Warrick, G. S. D.; DiNardo, S. Diminished Jak/STAT Signaling Causes Early-Onset Aging Defects in Stem Cell Cytokinesis. *Curr Biol* **2019**, *29* (2), 256-267.e253. DOI: 10.1016/j.cub.2018.11.064.
- (29) Bhaskar, P. K.; Southard, S.; Baxter, K.; Van Doren, M. Germline sex determination regulates sex-specific signaling between germline stem cells and their niche. *Cell Rep* **2022**, *39* (1), 110620. DOI: 10.1016/j.celrep.2022.110620.
- (30) Hasan, S.; Hétié, P.; Matunis, E. L. Niche signaling promotes stem cell survival in the *Drosophila* testis via the JAK-STAT target DIAP1. *Dev Biol* **2015**, *404* (1), 27-39. DOI: 10.1016/j.ydbio.2015.04.017.
- (31) Shields, A. R.; Spence, A. C.; Yamashita, Y. M.; Davies, E. L.; Fuller, M. T. The actin-binding protein profilin is required for germline stem cell maintenance and germ cell enclosure by somatic cyst cells. *Development* **2014**, *141* (1), 73-82. DOI: 10.1242/dev.101931.
- (32) Xing, Y.; Larson, K.; Li, J.; Li, W. X. Canonical and non-canonical functions of STAT in germline stem cell maintenance. *Dev Dyn* **2023**. DOI: 10.1002/dvdy.576.
- (33) Kiger, A. A.; Jones, D. L.; Schulz, C.; Rogers, M. B.; Fuller, M. T. Stem cell self-renewal specified by JAK-STAT activation in response to a support cell cue. *Science* **2001**, *294* (5551), 2542-2545.
- (34) Betz, A.; Lampen, N.; Martinek, S.; Young, M. W.; Darnell, J. E., Jr. A *Drosophila* PIAS homologue negatively regulates stat92E. *Proc Natl Acad Sci U S A* **2001**, *98* (17), 9563-9568.
- (35) Yamada, S.; Shiono, S.; Joo, A.; Yoshimura, A. Control mechanism of JAK/STAT signal transduction pathway. *FEBS Lett* **2003**, *534* (1-3), 190-196. DOI: 10.1016/s0014-5793(02)03842-5.
- (36) Liau, N. P. D.; Laktyushin, A.; Lucet, I. S.; Murphy, J. M.; Yao, S.; Whitlock, E.; Callaghan, K.; Nicola, N. A.; Kershaw, N. J.; Babon, J. J. The molecular basis of JAK/STAT inhibition by SOCS1. *Nat Commun* **2018**, *9* (1), 1558. DOI: 10.1038/s41467-018-04013-1.

- (37) Zi, Z.; Cho, K. H.; Sung, M. H.; Xia, X.; Zheng, J.; Sun, Z. In silico identification of the key components and steps in IFN-gamma induced JAK-STAT signaling pathway. *FEBS Lett* **2005**, *579* (5), 1101-1108. DOI: 10.1016/j.febslet.2005.01.009.
- (38) Issigonis, M.; Tulina, N.; de Cuevas, M.; Brawley, C.; Sandler, L.; Matunis, E. JAK-STAT signal inhibition regulates competition in the Drosophila testis stem cell niche. *Science* **2009**, *326* (5949), 153-156. DOI: 10.1126/science.1176817.
- (39) Voog, J.; D'Alterio, C.; Jones, D. L. Multipotent somatic stem cells contribute to the stem cell niche in the Drosophila testis. *Nature* **2008**, *454* (7208), 1132-1136.
- (40) Dutta, P.; Nath, S.; Li, J.; Li, W. X. Drosophila SERTAD domain protein Taranis is required in somatic cells for maintenance of male germline stem cells. *Dev Dyn* **2021**, *250* (2), 237-248. DOI: 10.1002/dvdy.255.
- (41) Xing, Y.; Li, W. X. Heterochromatin components in germline stem cell maintenance. *Sci Rep* **2015**, *5*, 17463. DOI: 10.1038/srep17463 From NLM.
- (42) Binari, R.; Perrimon, N. Stripe-specific regulation of pair-rule genes by hopscotch, a putative Jak family tyrosine kinase in Drosophila. *Genes Dev* **1994**, *8* (3), 300-312.
- (43) Luo, H.; Asha, H.; Kockel, L.; Parke, T.; Mlodzik, M.; Dearolf, C. R. The Drosophila Jak kinase hopscotch is required for multiple developmental processes in the eye. *Dev Biol* **1999**, *213* (2), 432-441.
- (44) Luo, H.; Hanratty, W. P.; Dearolf, C. R. An amino acid substitution in the Drosophila hopTum-I Jak kinase causes leukemia-like hematopoietic defects. *EMBO J* **1995**, *14* (7), 1412-1420. DOI: 10.1002/j.1460-2075.1995.tb07127.x.
- (45) Yan, R.; Small, S.; Desplan, C.; Dearolf, C. R.; Darnell, J. E., Jr. Identification of a Stat gene that functions in Drosophila development. *Cell* **1996**, *84* (3), 421-430.
- (46) Harrison, D. A.; Binari, R.; Nahreini, T. S.; Gilman, M.; Perrimon, N. Activation of a Drosophila Janus kinase (JAK) causes hematopoietic neoplasia and developmental defects. *Embo J* **1995**, *14* (12), 2857-2865.

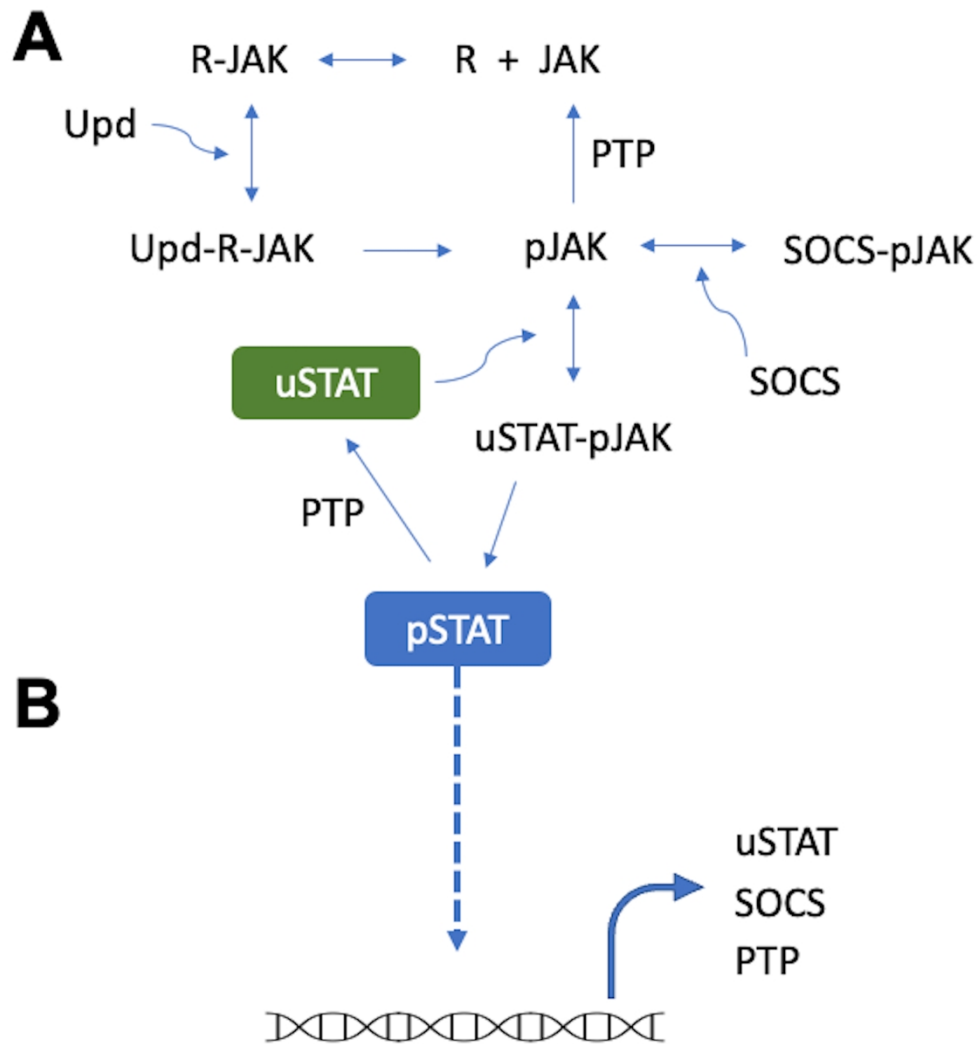
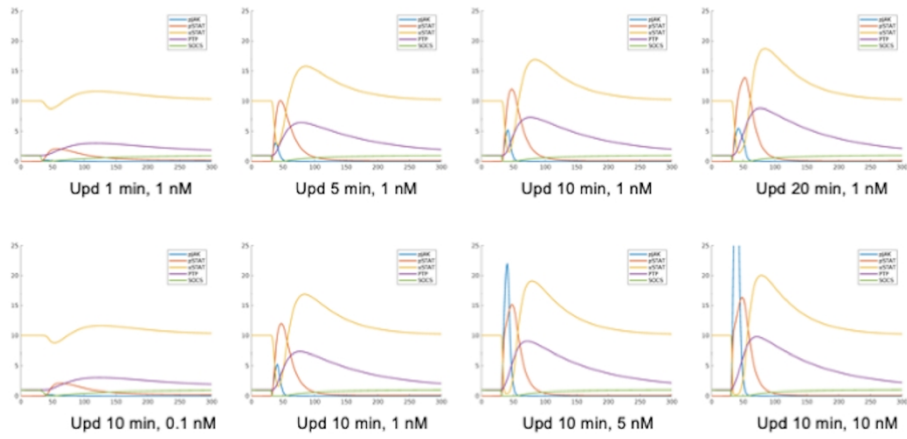
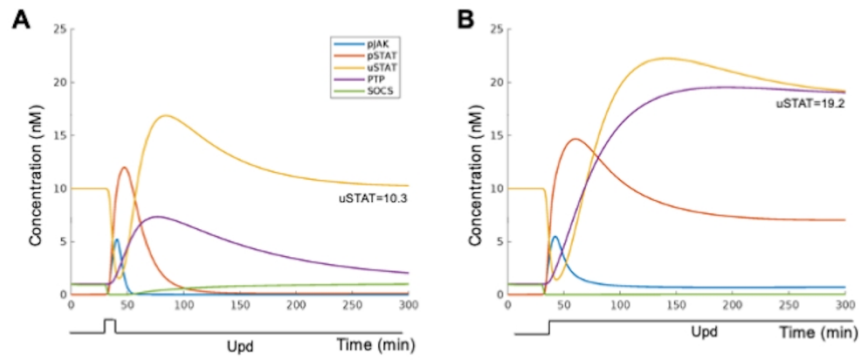


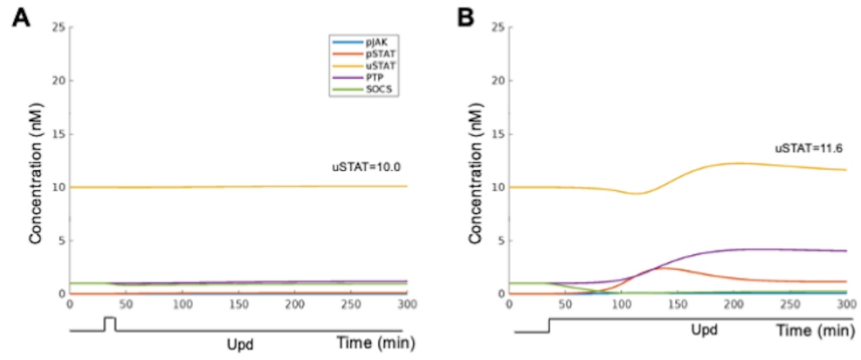
Figure 2



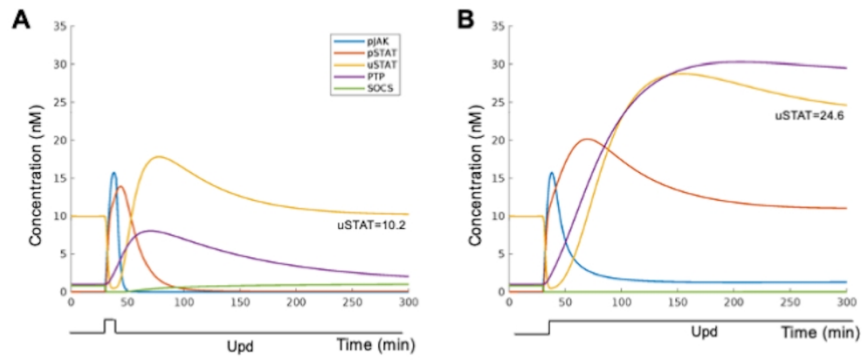
340x191mm (300 x 300 DPI)



340x191mm (300 x 300 DPI)

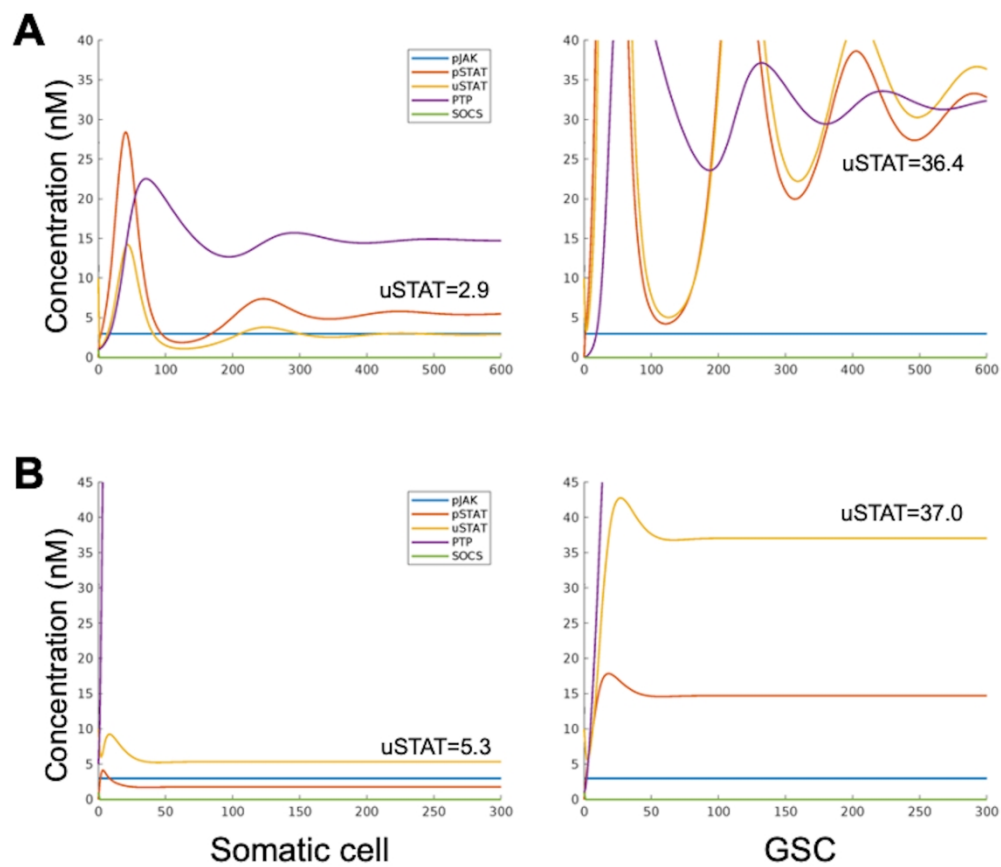


340x191mm (300 x 300 DPI)



340x191mm (300 x 300 DPI)

Figure 6



1586x1532mm (72 x 72 DPI)